Table 1. Immunization and treatment

Group	Monkeys (MM nos.)	Treatment		
		rIFN-γ[a]	Placebo[b]	SHIV-NI[c]
A	348, 352, 295	×		
B	316, 328		×	
C	371, 291, 413, 414	×		×
D	367, 369, 405, 411, 412		×	×

[a] 1×10^6 U, i.m. three times per week for 4 weeks.
[b] i.m.
[c] 1×10^5 $TCID_{50}$, i.v.

ent centrifugation. Freshly isolated PBMCs were used for ELISPOT assay and NK assay as described below. All plasma samples were frozen at −80 C until use.

Quantification of plasma viral RNA loads. Plasma viral RNA loads were determined by quantitative RT-PCR (50). Total RNAs were prepared from plasma with a QIAamp viral RNA kit (QIAGEN) according to the manufacturer's recommendations, and RT-PCR was performed using a *Taq*man RT-PCR kit (Perkin Elmer). RNAs of attenuated viruses and challenge virus were evaluated with primer pairs specific to SHIV NM-3rN and SHIV-C2/1, respectively, as previously described (14). These reactions were performed with a Prism 7700 Sequence Detector (Applied Biosystems, Foster City, Calif., U.S.A.) and analyzed using the manufacturer's software. For each run, a standard curve was generated from duplicate samples at different dilutions whose copy numbers were known, and the RNA in the plasma samples were quantified based on the copy number of the standard samples.

Measurement of antibodies to HIV-1 Env protein in plasma. HIV-1 Env-specific IgG antibodies in the plasma were detected by ELISA using the following method developed at Japan Immunoresearch Laboratories, Takasaki, Japan (2). In brief, a 96-well microplate (Nunc-Immuno™Modules, Maxisorp™, Nalge-Nunc, Rochester, N.Y., U.S.A.) was coated with HIV-1 IIIB gp160 recombinant viral protein (Advanced Biotechnologies, Inc., Columbia, Md., U.S.A.) at 1 μg/ml in 0.1 M Na_2CO_3-$NaHCO_3$ buffer (pH 9.6), incubated overnight at 4 C, washed with 0.15 M NaCl containing 0.05% Tween 20 and treated with 25% Block Ace™ (Nacalai Tesque, Inc., Kyoto, Japan) for 2 hr at room temperature, incubated overnight with plasma diluted with staining buffer (10% Block Ace) at 4 C, washed, incubated with peroxidase-conjugated goat anti-monkey IgG (1 μg/ml) (Kirkegaard & Perry Laboratories, Inc., Gaithersburg, Nd., U.S.A.) for 2 hr at room temperature, washed, treated with *O*-phenylenediamine dihydrochloride (OPD, Sigma, St. Louis, Mo., U.S.A.) for 10 min and immersed in 2 N H_2SO_4 to stop the reaction. Specific absorbances were read at 490 nm with a microplate reader as described (2). The amounts of antibody were expressed as the optical density. Plasmas of SHIV-infected monkeys and naïve monkeys were used as positive and negative controls, respectively.

IFN-γ ELISPOT assay. The number of antigen specific cytokine rIFN-γ-producing cells was determined with an IFN-γ ELISPOT kit (Mabtech, Nacka, Sweden) using an MAHAS4510 multi-screen 96-well plate (Millipore, Bedford, Mass., U.S.A.), anti-monkey IFN-γ antibody, biotinylated anti-IFN-γ antibody and streptavidin-alkaline phosphatase conjugate antibody, according to the manufacturer's instructions. SIV Gag p27 protein (soluble native p27, Advanced biotechnologies) was added to the cultures at a final concentration of 10 μg/ml. Medium alone was used as a negative control. As a positive control, concanavalin A was added to control wells at a final concentration of 5 μg/ml. Cells were tested at 1×10^6 cells per well in duplicate and incubated undisturbed at 37 C, 5% CO_2, for 36 hr. The resulting spots were counted with a microscope. Date in the figures show the mean number of spot-forming cells (SFC) per 1×10^6 PBMCs.

Flow cytometry. An absolute cell count was determined from samples of PBMCs as described previously (13). PBMCs of each monkey were stained with FITC-conjugated anti-monkey CD3 (FN-18; BioSource International, Belgium), phycoerythrin (PE)-conjugated anti-human CD4 (NU-TH/I; Nichirei), PerCP-conjugated anti-human CD8 (leu-2a; BD Pharmingen, San Diego, Calif., U.S.A.) or FITC-conjugated anti-human CD29 (4B4; Beckman Coulter). After hemolysis of the whole blood using FACS TM Lysing Solution (BD Pharmingen), each type of labeled lymphocytes was measured on a FACScan (Becton Dickinson, Mountain View, Calif., U.S.A.) by using Cell Quest software (Becton Dickinson). Absolute lymphocyte counts in the blood were determined with an automated blood cell counter (F-820; Sysmex, Japan).

NK cytotoxicity assay. NK cell activities of PBMCs in each monkey were periodically measured by a chromium (^{51}Cr) release assay using K562 cells as target cells (12). Briefly, PBMCs obtained from each mon-

key were used as effector cells. Serial dilutions of effector cells were cultured with 1×10^4 cells of ^{51}Cr-labeled K562 cells dispensed in triplicate into each well of 96-well plates. After 4 hr, the culture supernatants of each well were monitored with a γ counter. Cytotoxic activity was calculated as the percent specific lysis at an effector cells to target cells ratio of 50:1. Percent specific lysis was calculated from (experimental release−spontaneous release)/(total release−spontaneous release)×100. Total release was determined by treating the target cells with 2.5% Triton X-100.

Measurement of cytokines and CC-chemokines. PBMCs obtained from each monkey were incubated in a tissue-culture dish for 1 hr and were separated into adherent and non-adherent cells. We used peripheral blood lymphocytes (PBLs), prepared as non-adherent cells, in the cytokine and CC-chemokine detection assays. After the stimulation of non-adherent cells with the SIV Gag p27 protein (Advanced Biotechnologies) at a final concentration of 10 μg/ml for 72 hr, the productions of IFN-γ, IL-4, IL-10, MIP-1α, MIP-1β, RANTES were measured in the culture supernatants using an immunoassay kit (BioSource International) and Quantikine (R & D Systems, Minneapolis, Minn., U.S.A.).

Results

No Antiviral Effect of rIFN-γ Administration to Unvaccinated Naïve Monkeys against SHIV-C2/1 Infection

First, to evaluate the antiviral effects of rIFN-γ without vaccination against a challenge virus, SHIV-C2/1, three of five unvaccinated monkeys (MM348, MM352 and MM295) were administered with rIFN-γ (group A) and the other two (MM316 and MM328) were administered with placebo (group B). rIFN-γ was administered at a dose of 1×10^6 U per monkey three times per week for 4 weeks. Then these monkeys were challenged intravenously with 200 $TCID_{50}$ of a pathogenic SHIV-C2/1. The five challenged monkeys were monitored for viral load for 15 weeks.

As shown in Fig. 1-A, in placebo-administered naïve monkeys (group B) that were infected with SHIV-C2/1, the viral RNA loads in plasma dramatically increased to about 6.3×10^7 to 8.7×10^8 at 2 weeks post challenge (w.p.c.). On the other hand, in rIFN-γ-administered monkeys (group A), the viral RNA loads in plasma increased to about 1.6×10^7 at 2 w.p.c. Thus, the peaks of plasma viral load were reduced about 5-fold in group A monkeys with rIFN-γ compared with the levels in naïve group B monkeys. In both group A and group B, almost all monkeys developed a rapid and complete loss of $CD4^+$ T cells, but only one monkey in group A (MM 295) did not show complete loss of $CD4^+$ T cells. Viral set point levels of 4.6×10^6 to 5.0×10^5 copies/ml were maintained in these unvaccinated monkeys. These results show that rIFN-γ administration had little or no antiviral effects.

Enhanced Protective Effect of rIFN-γ Administration to Vaccinated Monkeys against SHIV-C2/1 Replication

To investigate the adjuvant effect of IFN-γ, nine monkeys were immunized with SHIV-NI. Four of them (MM371, MM291, MM413 and MM414) were administered with rIFN-γ (group C) and the other five monkeys (MM367, MM369, MM405, MM411, MM412) were administered with placebo (group D). The dose and schedule of rIFN-γ administration were the same with those of group A. Then these monkeys were challenged with SHIV-C2/1.

Neither the rIFN-γ administered monkeys (group C) nor the placebo-administered monkeys (group D) experienced the severe $CD4^+$ T cell loss after SHIV-C2/1 challenge that occurred in the unvaccinated monkeys (Fig. 2-B). However, the plasma viral RNA loads after the challenge were different in the two groups. In one rIFN-γ-administered monkey (MM413, group C), viral loads were undetectable after the challenge. In the three other rIFN-γ-administered monkeys (group C), the viral RNA loads in plasma quantified by PCR specific for a challenge SHIV-C2/1 were about 1×10^3 to 2×10^5 at 2 w.p.c. (Fig. 1-B). On the other hand, the plasma viral RNA loads increased to about 3×10^7 to 1×10^6 at 2 w.p.c. in placebo-administered monkeys (group D). Thus, in the vaccinated monkeys with rIFN-γ (group C), the peaks of plasma viral load were reduced 100- to 1,000-fold compared to those in the vaccinated monkeys without rIFN-γ (group D). The significant difference of the peak values of plasma viral load between groups C and D showed that vaccination of SHIV-NI in combination with rIFN-γ administration could induce strong resistance to SHIV-C2/1 replication.

Enhancement of IFN-γ Producing Cells in the Vaccinated Monkeys with rIFN-γ

To investigate whether IFN-γ augments the immune response induced by vaccination with a live attenuated SHIV, the number of virus specific spot forming cells (SFC) secreting IFN-γ of PBMCs in each monkey groups were measured by ELISPOT assays.

SIV Gag-specific SFC induced in the SHIV-NI vaccinated monkeys receiving rIFN-γ (group C) was higher than that induced in the vaccinated monkeys without rIFN-γ. Two weeks after the challenge, group C with rIFN-γ reached the highest number of Gag-specific IFN-γ SFC (Fig. 3-B). On the other hand, in the unvac-

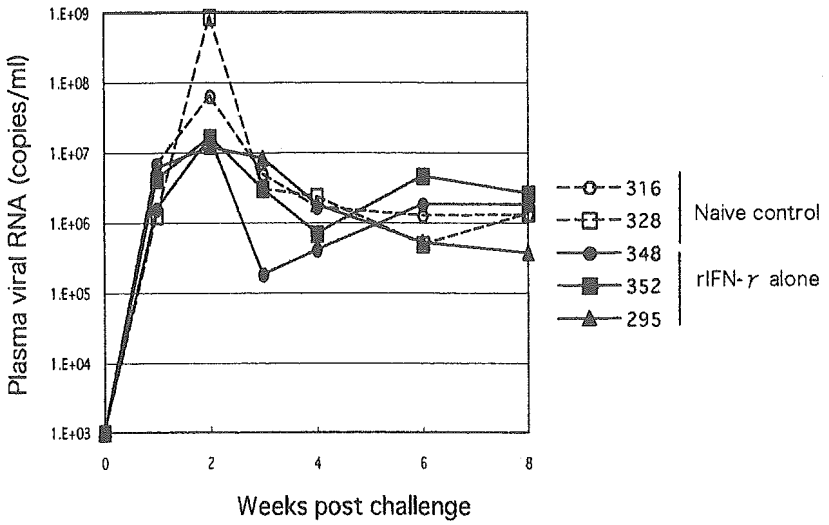

(A) Unvaccinated monkeys.

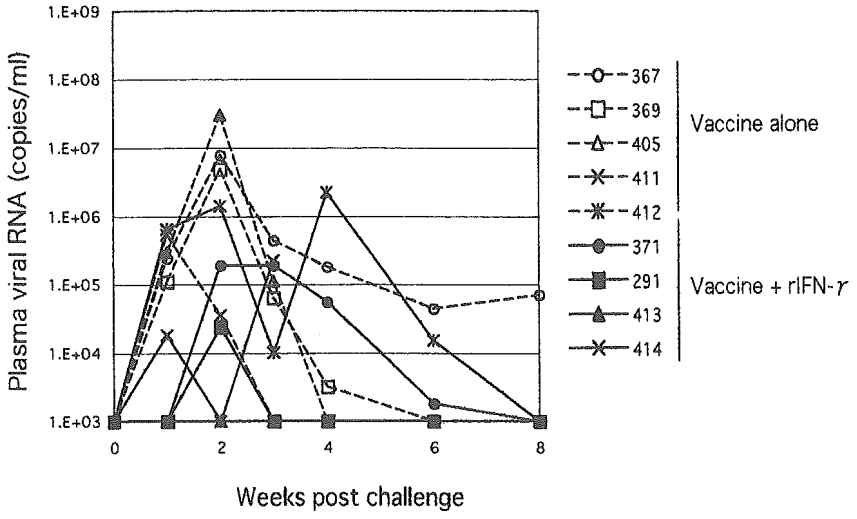

(B) Vaccinated monkeys.

Fig. 1. Kinetics of plasma viral RNA of the SHIV C2/1-infected monkeys. (A) Unvaccinated monkeys; (B) vaccinated monkeys. The experimental schedule of each group of monkeys is presented in Table 1.

cinated monkeys with and without rIFN-γ (groups A and B), the number of Gag-specific IFN-γ SFC were hardly detectable (Fig. 3-A). These results demonstrated that vaccination of SHIV-NI in combination with rIFN-γ administration augments the cellular immune (Th1) response.

Delayed Antibody Response in the SHIV-NI Vaccinated Monkeys Receiving rIFN-γ

The time of appearance of HIV-1 Env-specific IgG antibodies detected by ELISA was different in vaccinated macaques with and without rIFN-γ after the challenge (Fig. 4). The SHIV-NI-vaccinated monkeys that received the placebo (group D) exhibited HIV-1 gp160-specific IgG antibody responses gradually from 1 w.p.c. On the other hand, at 1 w.p.c. no antibody was detected in the SHIV-NI vaccinated monkeys that received rIFN-γ (MM291, MM413 and MM414) (group C). At 2 w.p.c. the titer of antibody dramatically increased in both monkey groups but was slightly higher in group D without rIFN-γ than in group C with rIFN-γ, which showed a higher Th1 response as shown in the previous section. No HIV-1 Env-specific IgG antibodies were detected in any of the vaccinated macaques before challenge (the cut off value was 0.11).

Enhanced Chemokine MIP-1α Production in the SHIV-NI Vaccinated Monkeys Receiving rIFN-γ

To assess the production of CC-hemokines and cytokines by antigen-stimulated PBMCs from the vacci-

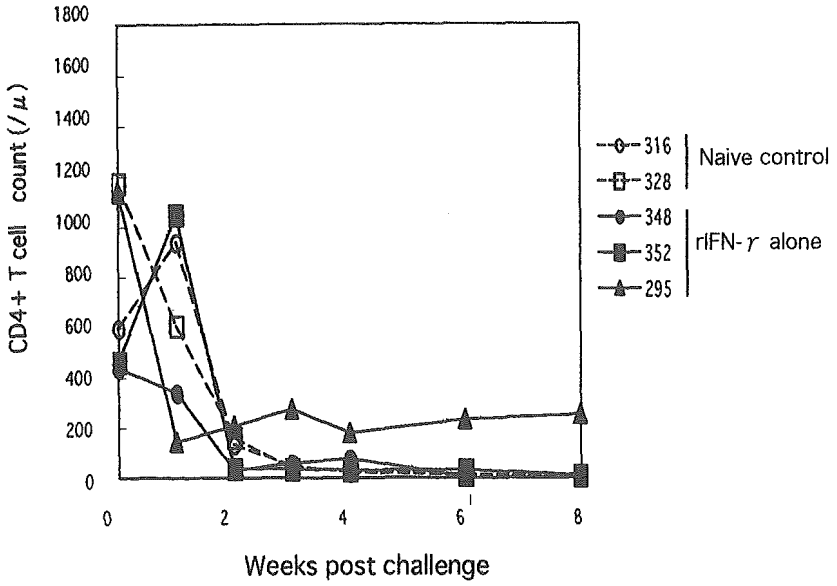

(A) Unvaccinated monkeys.

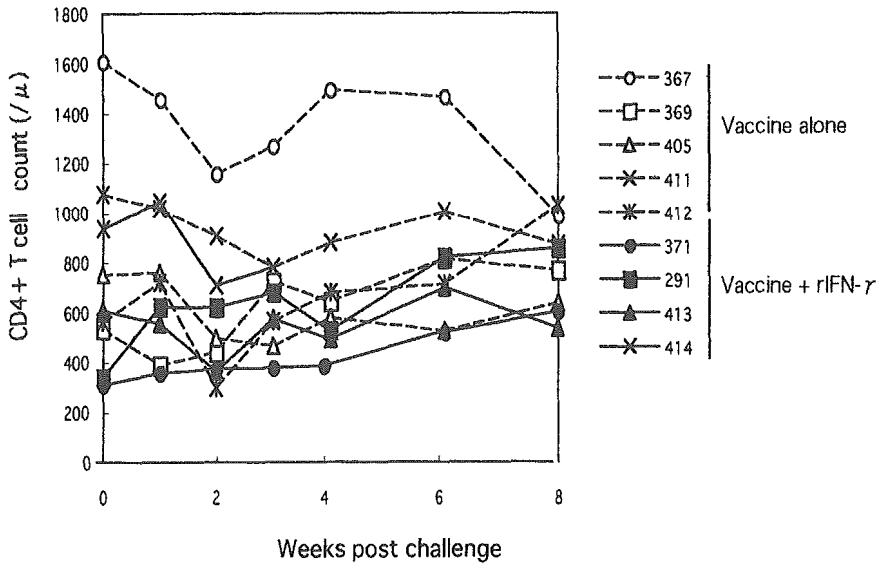

(B) Vaccinated monkeys.

Fig. 2. Changes in $CD4^+$ T cell counts in PBMCs of unvaccinated monkeys (A) and SHIV-NI-vaccinated monkeys (B) after SHIV C2/1 challenge.

nated monkeys (groups C and D), the production of MIP-1α, MIP-1β, RANTES, IFN-γ, IL-4 and IL-10 by specific ELISAs was analyzed. PBMCs of nine vaccinated monkeys (groups C and D) were stimulated with SIV Gag and their presence in cell culture supernatants were measured before and at 2 weeks after vaccination.

No substantial differences were seen in the production of MIP-1β, RANTES, IFN-γ, IL-4 or IL-10 by PBMCs stimulated with SIV Gag in the SHIV-NI vaccinated monkeys with and without rIFN-γ during the time of follow-up (data not shown). However, the levels of MIP-1α secreted by PBMCs in SHIV-NI-vaccinated monkeys receiving rIFN-γ (group C) were dramatically higher at 2 week post vaccination (w.p.v.), than those of vaccinated monkeys without rIFN-γ (group D) (Fig. 5).

Augmentation of NK Activity by rIFN-γ Administration

To evaluate innate immune response that contributed to the protection against SHIV-C2/1, we assayed NK cell activity of PBMCs of the SHIV-NI vaccinated monkeys with (group C) and without (group D) rIFN-γ.

In all the group C monkeys except MM291, NK cell

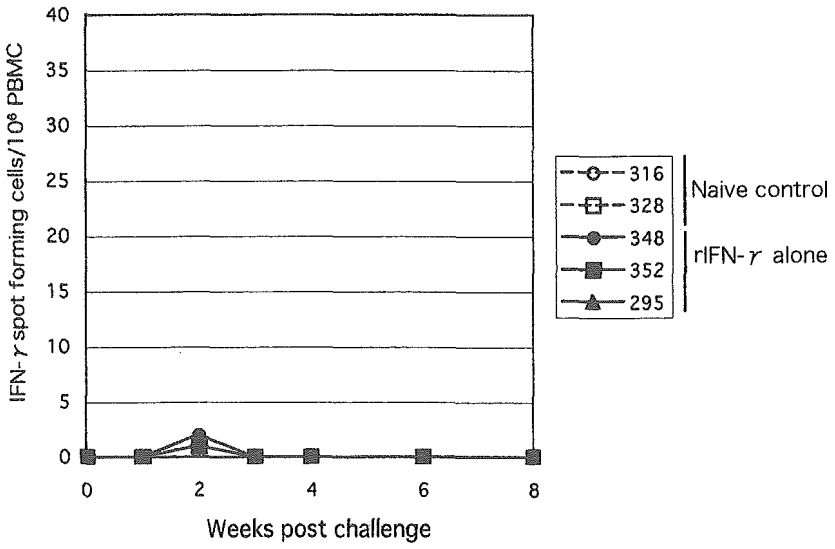

(A) Unvaccinated monkeys.

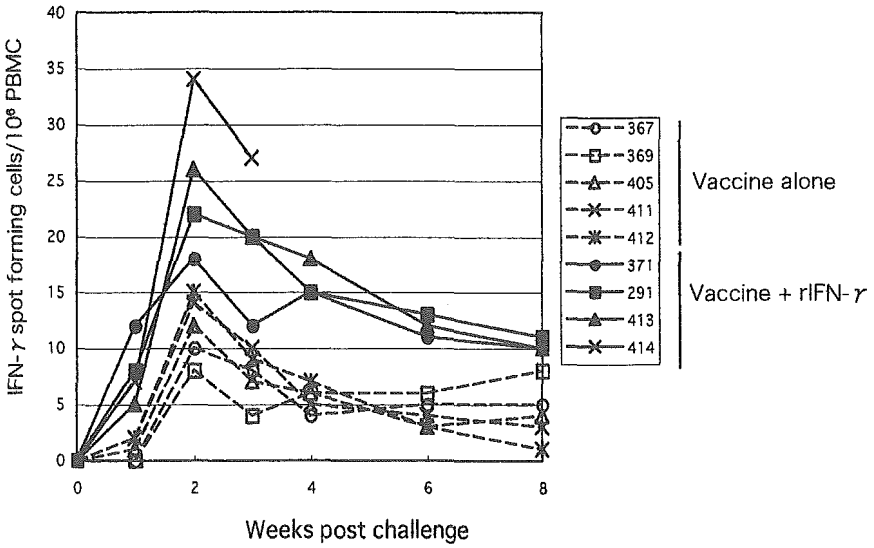

(B) Vaccinated monkeys.

Fig. 3. Numbers of SIV Gag-specific IFN-γ-producing cells in PBMCs of unvaccinated monkeys (A) and vaccinated monkeys (B). PBMCs were stimulated with SIV Gag protein. IFN-γ-producing cells were detected by IFN-γ-specific ELISPOT assays, and data are expressed as the number of SFC per 10^6 cells. Each point represents the mean number of IFN-γ spots in duplicate wells.

activities at 1 w.p.v. were approximately 30 to 45% greater than the activities before rIFN-γ treatment (Fig. 6). These augmented NK activities were observed during the 3-week rIFN-γ treatment period. On the other hand, no augmentation was observed in the vaccinated monkeys without IFN-γ (group D). After the challenge, The NK activities of these monkeys remained at low levels in both groups. These results demonstrate that rIFN-γ administration augmented NK cell activities in the vaccinated monkeys.

Discussion

We previously reported that monkeys immunized with a nef-deleted SHIV-NM-3rN (SHIV-NI) or an SHIV-NI expressing human IFN-γ (SHIV-IFN-γ) could control the replication of a heterologous pathogenic virus and prevent the loss of $CD4^+$ T cells. SHIV-IFN-γ vaccinated monkeys showed resistance to the SHIV C2/1 challenge, even though only 4 weeks had passed

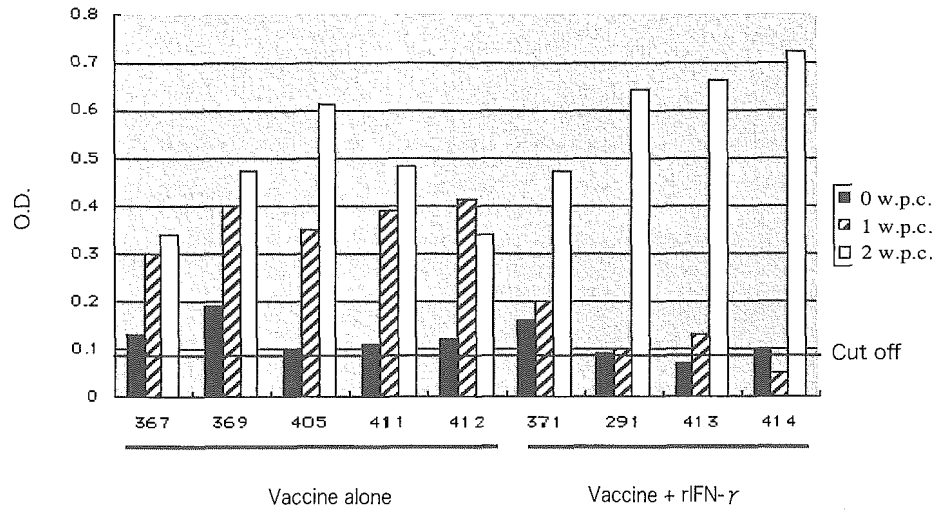

Fig. 4. HIV-1 Env-specific IgG antibodies in plasma of SHIV-NI vaccinated monkeys combined with rIFN-γ or placebo administration after challenge.

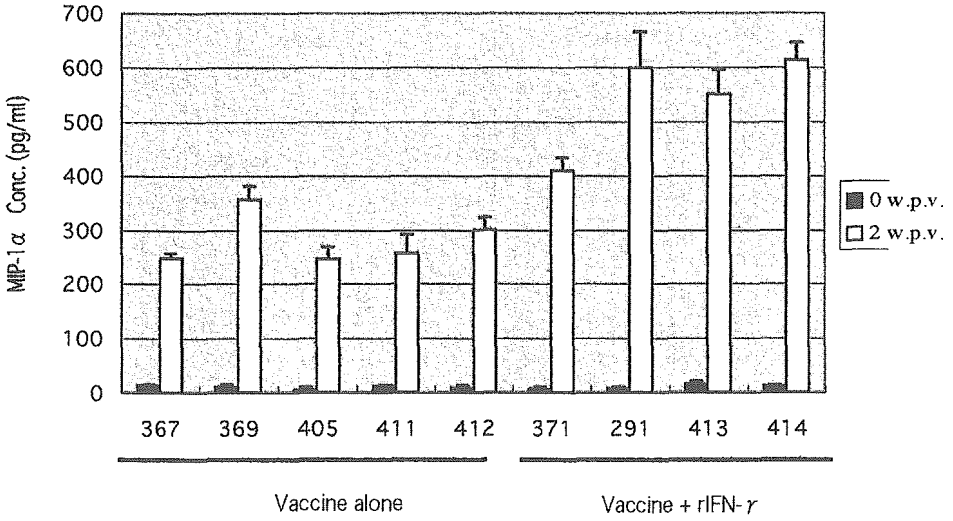

Fig. 5. Production of MIP-1α by SIV Gag-stimulated PBMCs of SHIV-NI vaccinated monkeys combined with rIFN-γ or placebo. PBMCs were obtained prior to vaccination (0) and 2 weeks after vaccination.

since the immunization. Moreover, the peak value of the plasma viral load in the early phase of the challenge with SHIV-C2/1 was reduced in the SHIV-IFN-γ-vaccinated monkeys compared with those in the SHIV-NI vaccinated monkeys. These results raise the possibility that IFN-γ makes a strong contribution to the suppression of SHIV-C2/1 replication (13, 23). The other study has been reported that HIV p24 antigen was decreased in plasma samples obtained from six of nine rIFN-γ-administered patients with initially detectable HIV protein (19). These data suggest that rIFN-γ should be considered as a therapeutic agent, possibly with other antiviral, in the treatment of patients with AIDS. However, whether exogenous IFN-γ administration induces protective immunity in the SHIV/monkey model which is useful for clarifying the mechanism of IFN-γ-induced protection is unknown.

The aim of the present study was to investigate whether exogenous IFN-γ administration could augment the immune response induced by vaccination with a live attenuated SHIV-NI. In the vaccinated monkey groups, SHIV-NI vaccination combined with rIFN-γ administration resulted in significantly limiting the peak value of the plasma viral load and maintaining $CD4^+$ T cells after SHIV-C2/1 challenge. In this group, the peak of plasma viral load was reduced approximately 100- to 1,000-fold and the number of SIV Gag-specific IFN-γ-producing cells increased 2-fold compared with those in the SHIV-NI-vaccinated monkeys without rIFN-γ (group D). On the other hand, in the unvaccinat-

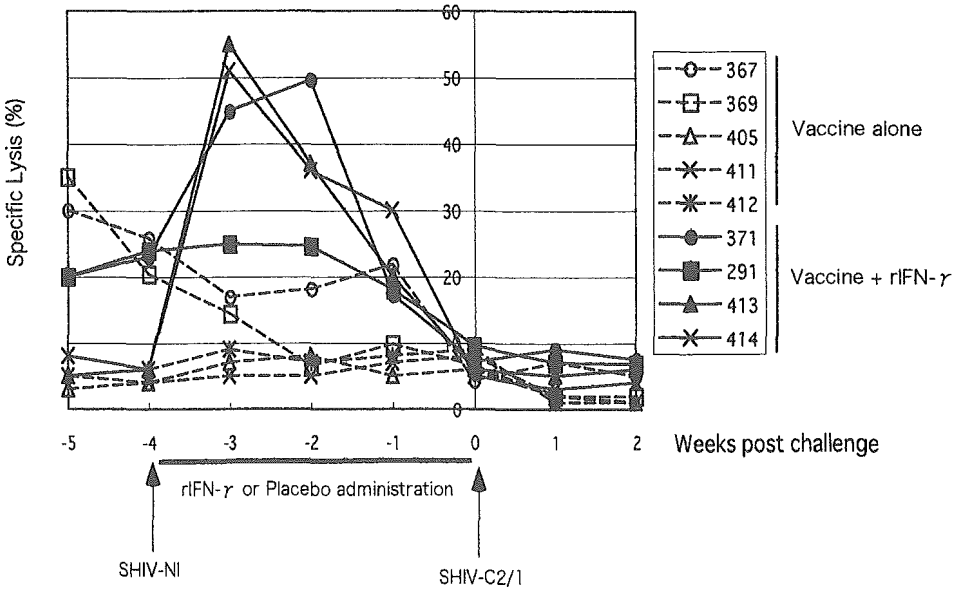

Fig. 6. NK cell activity of PBMCs in the SHIV-NI vaccinated monkeys combined with rIFN-γ or placebo administration before and after challenge.

ed monkey groups, $CD4^+$ T cells declined after SHIV-C2/1 infection almost equally in monkeys with rIFN-γ (group A) and without (group B). SIV Gag-specific IFN-γ-producing cells were undetectable in unvaccinated monkeys of both groups. The increase in the number of IFN-γ-producing cells in the vaccinated monkeys was closely correlated with the decrease in the peak value of plasma viral load of SHIV-C2/1.

These data suggest that vaccination with SHIV-NI in combination with rIFN-γ administration is more effective at modulating the immune system into the Th1-type response than either rIFN-γ administration alone or SHIV-NI vaccination alone. This modulation to a Th1-type response indicates that rIFN-γ administration could induce the strong cellular immune response against SHIV infection. The augmented Th1-type responses assessed by SIV Gag protein-specific IFN-γ-producing cell activity might be associated with the activity of cytotoxic T lymphocytes (CTLs). Antigen-specific Th1-mediated immune responses and CTLs have been reported to provide protection and reduce disease progression (16, 22, 32, 36, 39). Th1/$CD8^+$ T cell responses have been shown to play an important role in controlling HIV-1 replication (5, 27, 34, 35, 37, 38, 40, 42–44). Th1/$CD4^+$ T cell responses (antigen-specific $CD4^+$ T helper cells) also may promote CTL activity either by a CD4-antigen-presenting cell (APC)-CD8 pathway or by IL-2 secretion (20, 41, 57). The present observations are encouraging in light of the hypothesis that Th1-mediated immunity is associated with resistance to virus infection and suppression (3, 28).

To investigate whether IFN-γ affect the innate immunity, we examined production of CC-chemokines and cytokines, and the NK activity of freshly isolated PBMCs of these monkeys. The levels of RANTES, MIP-1α, MIP-1β, IFN-γ, IL-4 and IL-10 of supernatants from SIV Gag-stimulated PBMCs were measured by ELISA. In result of these, NK activity and MIP-1α production were enhanced in SHIV-NI-vaccinated monkeys with rIFN-γ (group C). Moreover, no HIV-1 Env-specific antibody was detected at 1 w.p.c. in SHIV-NI-vaccinated monkeys with rIFN-γ. On the other hand, SHIV-NI vaccinated monkeys without rIFN-γ (group D) exhibited HIV-1 Env-specific antibody responses at 1 w.p.c. The lower IgG Ab response generated in SHIV-NI vaccinated monkeys with rIFN-γ might have resulted from the predominant Th1>Th2 cytokine response modulated probably by both NK activity and MIP-1α production. Several studies have shown that MIP-1α stimulation enhances IFN-γ production, which is essential for the induction of Th1-derived HIV-specific cell-mediated immunity (25). MIP-1α was reported to activate NK cells and the activated NK cells produce MIP-1α (29, 31, 45). NK cells are a critical component of the host innate immune response to a variety of viruses, fungi, parasites and bacteria (35, 45, 52). After activation, NK cells release various cytokines and chemokines including MIP-1α that induce the inflammatory response, modulate hematopoiesis, control monocyte and granulocyte growth and function, and influence the type of adaptive immune responses (52). With regard to HIV infection, the nonspecificity of NK cell activity might be relevant to the maintenance of a degree of antiviral activity in the

face of a high level of virus replication that negatively impacts HIV-specific cellular and humoral immune responses (7, 15). Recently, Enose et al. (13) showed vaccination of monkeys with live attenuated SHIV having IFN-γ effectively suppressed the peak value of plasma viral loads from 1 to 3 weeks after SHIV-C2/1 challenge. Cellular immune responses were augmented by SHIV-IFN-γ as compared to SHIV-NI without the IFN-γ gene insert. From 4 to 12 weeks after the challenge, however, these monkeys showed a transient increase in viral load. IFN-γ mediated inflammation has been reported to be associated with a lack of protection from SIV challenge in vaccinated rhesus macaques (1). It is possible that IFN-γ-driven inflammation promotes SHIV-C2/1 replication in SHIV-IFN-γ immunized monkeys at later stage, because SHIV-IFN-γ immunization may increase IFN-γ mRNA levels in lymphoid tissues (1). In a vaccine study using a combination of DNA immunization with plasmid adjuvants expressing GM-CSF and IFN-γ (30), both humoral and cellular immune responses to SIV antigens were augmented by cytokine expression plasmids as compared to mock plasmid without a cytokine gene insert, but the plasma viral loads at set points were not significantly different between both the immunized group and the non-immunized control group. On the other hand, in this present study, the SHIV-NI-vaccinated monkeys that were treated with rIFN-γ (group C) exhibited various responses including augmentation of HIV-1 Env-specific antibody responses. In addition, the innate and cellular immune responses in these monkeys significantly reduced the peak value of the plasma viral load without a transient increase in viral RNA load after the challenge. To obtain better protection against a pathogenic virus, it may be necessary to develop a vaccine that induces both innate and cellular immune responses.

In conclusion, our data show that SHIV-NI vaccination combined with rIFN-γ administration induces strong SIV Gag-specific Th1-type cellular immune response, which might contribute to the control of a heterologous pathogenic SHIV challenge infection. Since the magnitude of the induced immunity is considered enough for protection against viral infection and disease progression, rIFN-γ could be used as an adjuvant for attenuated vaccine candidates against SHIV infection, probably against HIV infection.

We thank James Raymond for English editing of this manuscript. We are grateful to Ms. Ai Himeno and Ms. Humiko Ogatu for technical assistance. This work was supported by a Grant-in-Aid for Scientific Research from the Ministry of Education, Culture, Sports, Science and Technology, Japan and a Research Grant on Health Sciences focusing on Drug Innovation from the Japan Health Sciences Foundation. K.K. is supported by the 21st Century COE Program of the Ministry of Education, Culture, Sports, Science and Technology, Japan.

References

1) Abel, K., La Franco-Scheuch, L., Rourke, T., Ma, Z.M., De Silva, V., Fallert, B., Beckett, L., Reinhart, T.A., and Miller, C.J. 2004. Gamma interferon-mediated inflammation is associated with lack of protection from intravaginal simian immunodeficiency virus SIVmac239 challenge in simian-human immunodeficiency virus 89.6-immunized rhesus macaques. J. Virol. **78**: 841–854.
2) Akagi, T., Kawamura, M., Ueno, M., Hiraishi, K., Adachi, M., Serizawa, T., Akashi, M., and Baba, M. 2003. Mucosal immunization with inactivated HIV-1-capturing nanospheres induces a significant HIV-1-specific vaginal antibody response in mice. J. Med. Virol. **69**: 163–172.
3) Bailer, R.T., Holloway, A., Sun, J., Margolick, J.B., Martin, M., Kostman, J., and Montaner, L.J. 1999. IL-13 and IFN-gamma secretion by activated T cells in HIV-1 infection associated with viral suppression and a lack of disease progression. J. Immunol. **162**: 7534–7542.
4) Benito, J.M., Lopez, M., and Soriano, V. 2004. The role of CD8+ T-cell response in HIV infection. AIDS Rev. **6**: 79–88.
5) Bernard, N.F., Yannakis, C.M., Lee, J.S., and Tsoukas, C.M. 1999. Human immunodeficiency virus (HIV)-specific cytotoxic T lymphocyte activity in HIV-exposed seronegative persons. J. Infect. Dis. **179**: 538–547.
6) Billiau, A. 1998. Interferon-gamma, the TH1/TH2 paradigm in autoimmunity. Bull. Mem. Acad. R. Med. Belg. **153**: 231–233.
7) Bluman, E.M., Bartynski, K.J., Avalos, B.R., and Caligiuri, M.A. 1996. Human natural killer cells produce abundant macrophage inflammatory protein-1 alpha in response to monocyte-derived cytokines. J. Clin. Invest. **97**: 2722–2727.
8) Chatterjee, S., and Hunter, E. 1987. Recombinant human interferons inhibit replication of Mason-Pfizer monkey virus in primate cells. Virology **157**: 548–551.
9) Connor, R.I., Montefiori, D.C., Binley, J.M., Moore, J.P., Bonhoeffer, S., Gettie, A., Fenamore, E.A., Sheridan, K.E., Ho, D.D., Dailey, P.J., and Marx, P.A. 1998. Temporal analyses of virus replication, immune responses, and efficacy in rhesus macaques immunized with a live, attenuated simian immunodeficiency virus vaccine. J. Virol. **72**: 7501–7509.
10) Constantoulakis, P., Campbell, M., Felber, B.K., Nasioulas, G., Afonina, E., and Pavlakis, G.N. 1993. Inhibition of Rev-mediated HIV-1 expression by an RNA binding protein encoded by the interferon-inducible 9-27 gene. Science **259**: 1314–1318.
11) Daniel, M.D., Kirchhoff, F., Czajak, S.C., Sehgal, P.K., and Desrosiers, R.C. 1992. Protective effects of a live attenuated SIV vaccine with a deletion in the nef gene. Science **258**: 1938–1941.
12) De Maria, A., Fogli, M., Costa, P., Murdaca, G., Puppo, F., Mavilio, D., Moretta, A., and Moretta, L. 2003. The

impaired NK cell cytolytic function in viremic HIV-1 infection is associated with a reduced surface expression of natural cytotoxicity receptors (NKp46, NKp30 and NKp44). Eur. J. Immunol. **33**: 2410–2418.
13) Enose, Y., Kita, M., Yamamoto, T., Suzuki, H., Miyake, A., Horiuchi, R., Ibuki, K., Kaneyasu, K., Kuwata, T., Takahashi, E., Sakai, K., Shinohara, K., Miura, T., and Hayami, M. 2004. Protective effects of nef-deleted SHIV or that having IFN-gamma against disease induced with a pathogenic virus early after vaccination. Arch. Virol. **149**: 1705–1720.
14) Enose, Y., Ui, M., Miyake, A., Suzuki, H., Uesaka, H., Kuwata, T., Kunisawa, J., Kiyono, H., Takahashi, H., Miura, T., and Hayami, M. 2002. Protection by intranasal immunization of a nef-deleted, nonpathogenic SHIV against intravaginal challenge with a heterologous pathogenic SHIV. Virology **298**: 306–316.
15) Fehniger, T.A., Herbein, G., Yu, H., Para, M.I., Bernstein, Z.P., O'Brien, W.A., and Caligiuri, M.A. 1998. Natural killer cells from HIV-1+ patients produce C-C chemokines and inhibit HIV-1 infection. J. Immunol. **161**: 6433–6438.
16) Ferrari, C., Penna, A., Bertoletti, A., Cavalli, A., Missale, G., Lamonaca, V., Boni, C., Valli, A., Bertoni, R., Urbani, S., Scognamiglio, P., and Fiaccadori, F. 1998. Antiviral cell-mediated immune responses during hepatitis B and hepatitis C virus infections. Recent Results Cancer. Res. **154**: 330–336.
17) Giavedoni, L., Ahmad, S., Jones, L., and Yilma, T. 1997. Expression of gamma interferon by simian immunodeficiency virus increases attenuation and reduces postchallenge virus load in vaccinated rhesus macaques. J. Virol. **71**: 866–872.
18) Hartshorn, K.L., Neumeyer, D., Vogt, M.W., Schooley, R.T., and Hirsch, M.S. 1987. Activity of interferons alpha, beta, and gamma against human immunodeficiency virus replication *in vitro*. AIDS Res. Hum. Retroviruses **3**: 125–133.
19) Heagy, W., Groopman, J., Schindler, J., and Finberg, R. 1990. Use of IFN-gamma in patients with AIDS. J. Acquir. Immune Defic. Syndr. **3**: 584–590.
20) Heeney, J.L. 2002. The critical role of CD4 (+) T-cell help in immunity to HIV. Vaccine **20**: 1961–1963.
21) Huang, S., Hendriks, W., Althage, A., Hemmi, S., Bluethmann, H., Kamijo, R., Vilcek, J., Zinkernagel, R.M., and Aguet, M. 1993. Immune response in mice that lack the interferon-gamma receptor. Science **259**: 1742–1745.
22) Hukkanen, V., Broberg, E., Salmi, A., and Eralinna, J.P. 2002. Cytokines in experimental herpes simplex virus infection. Int. Rev. Immunol. **21**: 355–371.
23) Iida, T., Kuwata, T., Ui, M., Suzuki, H., Miura, T., Ibuki, K., Takahashi, H., Yamamoto, T., Imanishi, J., Hayami, M., and Kita, M. 2004. Augmentation of antigen-specific cytokine responses in the early phase of vaccination with a live-attenuated simian/human immunodeficiency chimeric virus expressing IFN-gamma. Arch. Virol. **149**: 743–757.
24) Johnson, R.P., Lifson, J.D., Czajak, S.C., Cole, K.S., Manson, K.H., Glickman, R., Yang, J., Montefiori, D.C., Montelaro, R., Wyand, M.S., and Desrosiers, R.C. 1999. Highly attenuated vaccine strains of simian immunodeficiency virus protect against vaginal challenge: inverse relationship of degree of protection with level of attenuation. J. Virol. **73**: 4952–4961.
25) Karpus, W.J., Lukacs, N.W., Kennedy, K.J., Smith, W.S., Hurst, S.D., and Barrett, T.A. 1997. Differential CC chemokine-induced enhancement of T helper cell cytokine production. J. Immunol. **158**: 4129–4136.
26) Karupiah, G., Blanden, R.V., and Ramshaw, I.A. 1990. Interferon gamma is involved in the recovery of athymic nude mice from recombinant vaccinia virus/interleukin 2 infection. J. Exp. Med. **172**: 1495–1503.
27) Kaul, R., Rowland-Jones, S.L., Kimani, J., Fowke, K., Dong, T., Kiama, P., Rutherford, J., Njagi, E., Mwangi, F., Rostron, T., Onyango, J., Oyugi, J., MacDonald, K.S., Bwayo, J.J., and Plummer, F.A. 2001. New insights into HIV-1 specific cytotoxic T-lymphocyte responses in exposed, persistently seronegative Kenyan sex workers. Immunol. Lett. **79**: 3–13.
28) Kostense, S., Vandenberghe, K., Joling, J., Van Baarle, D., Nanlohy, N., Manting, E., and Miedema, F. 2002. Persistent numbers of tetramer+ CD8 (+) T cells, but loss of interferon-gamma+ HIV-specific T cells during progression to AIDS. Blood **99**: 2505–2511.
29) Kottilil, S., Chun, T.W., Moir, S., Liu, S., McLaughlin, M., Hallahan, C.W., Maldarelli, F., Corey, L., and Fauci, A.S. 2003. Innate immunity in human immunodeficiency virus infection: effect of viremia on natural killer cell function. J. Infect. Dis. **187**: 1038–1045.
30) Lena, P., Villinger, F., Giavedoni, L., Miller, C.J., Rhodes, G., and Luciw, P. 2002. Co-immunization of rhesus macaques with plasmid vectors expressing IFN-gamma, GM-CSF, and SIV antigens enhances anti-viral humoral immunity but does not affect viremia after challenge with highly pathogenic virus. Vaccine **20** (Suppl 4): A69–79.
31) Loetscher, P., Seitz, M., Clark-Lewis, I., Baggiolini, M., and Moser, B. 1996. Activation of NK cells by CC chemokines. Chemotaxis, Ca^{2+} mobilization, and enzyme release. J. Immunol. **156**: 322–327.
32) Lusso, P. 2000. Chemokines and viruses: the dearest enemies. Virology **273**: 228–240.
33) Mason, R.D., Bowmer, M.I., Howley, C.M., and Grant, M.D. 2005. Cross-reactive cytotoxic T lymphocytes against human immunodeficiency virus type 1 protease and gamma interferon-inducible protein 30. J. Virol. **79**: 5529–5536.
34) Musey, L., Hughes, J., Schacker, T., Shea, T., Corey, L., and McElrath, M.J. 1997. Cytotoxic-T-cell responses, viral load, and disease progression in early human immunodeficiency virus type 1 infection. N. Engl. J. Med. **337**: 1267–1274.
35) Ogg, G.S., Jin, X., Bonhoeffer, S., Dunbar, P.R., Nowak, M.A., Monard, S., Segal, J.P., Cao, Y., Rowland-Jones, S.L., Cerundolo, V., Hurley, A., Markowitz, M., Ho, D.D., Nixon, D.F., and McMichael, A.J. 1998. Quantitation of HIV-1-specific cytotoxic T lymphocytes and plasma load of viral RNA. Science **279**: 2103–2106.
36) Ohga, S., Nomura, A., Takada, H., and Hara, T. 2002. Immunological aspects of Epstein-Barr virus infection. Crit. Rev. Oncol. Hematol. **44**: 203–215.
37) Pinto, L.A., Sullivan, J., Berzofsky, J.A., Clerici, M., Kessler, H.A., Landay, A.L., and Shearer, G.M. 1995. ENV-

specific cytotoxic T lymphocyte responses in HIV seronegative health care workers occupationally exposed to HIV-contaminated body fluids. J. Clin. Invest. **96**: 867–876.
38) Pontesilli, O., Klein, M.R., Kerkhof-Garde, S.R., Pakker, N.G., de Wolf, F., Schuitemaker, H., and Miedema, F. 1998. Longitudinal analysis of human immunodeficiency virus type 1-specific cytotoxic T lymphocyte responses: a predominant gag-specific response is associated with nonprogressive infection. J. Infect. Dis. **178**: 1008–1018.
39) Rico, M.A., Quiroga, J.A., Subira, D., Castanon, S., Esteban, J.M., Pardo, M., and Carreno, V. 2001. Hepatitis B virus-specific T-cell proliferation and cytokine secretion in chronic hepatitis B antibody-positive patients treated with ribavirin and interferon alpha. Hepatology **33**: 295–300.
40) Rinaldo, C., Huang, X.L., Fan, Z.F., Ding, M., Beltz, L., Logar, A., Panicali, D., Mazzara, G., Liebmann, J., Cottrill, M., et al. 1995. High levels of anti-human immunodeficiency virus type 1 (HIV-1) memory cytotoxic T-lymphocyte activity and low viral load are associated with lack of disease in HIV-1-infected long-term nonprogressors. J. Virol. **69**: 5838–5842.
41) Rosenberg, E.S., Billingsley, J.M., Caliendo, A.M., Boswell, S.L., Sax, P.E., Kalams, S.A., and Walker, B.D. 1997. Vigorous HIV-1-specific CD4+ T cell responses associated with control of viremia. Science **278**: 1447–1450.
42) Rowland-Jones, S.L., and McMichael, A. 1995. Immune responses in HIV-exposed seronegatives. Curr. Opin. Immunol. **7**: 448–455.
43) Rowland-Jones, S.L., Nixon, D.F., Aldhous, M.C., Gotch, F., Ariyoshi, K., Hallam, N., Kroll, J.S., Froebel, K., and McMichael, A. 1993. HIV-specific cytotoxic T-cell activity in an HIV-exposed but uninfected infant. Lancet **341**: 860–861.
44) Rowland-Jones, S., Sutton, J., Ariyoshi, K., Dong, T., Gotch, F., McAdam, S., Whitby, D., Sabally, S., Gallimore, A., Corrah, T., et al. 1995. HIV-specific cytotoxic T-cells in HIV-exposed but uninfected Gambian women. Nat. Med. **1**: 59–64.
45) Salazar-Mather, T.P., Hamilton, T.A., and Biron, C.A. 2000. A chemokine-to-cytokine-to-chemokine cascade critical in antiviral defense. J. Clin. Invest. **105**: 985–993.
46) Schmitz, J.E., Kuroda, M.J., Santra, S., Sasseville, V.G., Simon, M.A., Lifton, M.A., Racz, P., Tenner-Racz, K., Dalesandro, M., Scallon, B.J., Ghrayeb, J., Forman, M.A., Montefiori, D.C., Rieber, E.P., Letvin, N.L., and Reimann, K.A. 1999. Control of viremia in simian immunodeficiency virus infection by CD8+ lymphocytes. Science **283**: 857–860.
47) Shinohara, K., Sakai, K., Ando, S., Ami, Y., Yoshino, N., Takahashi, E., Someya, K., Suzaki, Y., Nakasone, T., Sasaki, Y., Kaizu, M., Lu, Y., and Honda, M. 1999. A highly pathogenic simian/human immunodeficiency virus with genetic changes in cynomolgus monkey. J. Gen. Virol. **80**: 1231–1240.
48) Sivori, S., Pende, D., Bottino, C., Marcenaro, E., Pessino, A., Biassoni, R., Moretta, L., and Moretta, A. 1999. NKp46 is the major triggering receptor involved in the natural cytotoxicity of fresh or cultured human NK cells. Correlation between surface density of NKp46 and natural cytotoxicity against autologous, allogeneic or xenogeneic target cells. Eur. J. Immunol. **29**: 1656–1666.
49) Stahl-Hennig, C., Gundlach, B.R., Dittmer, U., ten Haaft, P., Heeney, J., Zou, W., Emilie, D., Sopper, S., and Uberla, K. 2003. Replication, immunogenicity, and protective properties of live-attenuated simian immunodeficiency viruses expressing interleukin-4 or interferon-gamma. Virology **305**: 473–485.
50) Suryanarayana, K., Wiltrout, T.A., Vasquez, G.M., Hirsch, V.M., and Lifson, J.D. 1998. Plasma SIV RNA viral load determination by real-time quantification of product generation in reverse transcriptase-polymerase chain reaction. AIDS Res. Hum. Retroviruses **14**: 183–189.
51) Taylor, M.D., Korth, M.J., and Katze, M.G. 1998. Interferon treatment inhibits the replication of simian immunodeficiency virus at an early stage: evidence for a block between attachment and reverse transcription. Virology **241**: 156–162.
52) Trinchieri, G. 1989. Biology of natural killer cells. Adv. Immunol. **47**: 187–376.
53) Turner, P.K., Houghton, J.A., Petak, I., Tillman, D.M., Douglas, L., Schwartzberg, L., Billups, C.A., Panetta, J.C., and Stewart, C.F. 2004. Interferon-gamma pharmacokinetics and pharmacodynamics in patients with colorectal cancer. Cancer Chemother. Pharmacol. **53**: 253–260.
54) Ui, M., Kuwata, T., Igarashi, T., Ibuki, K., Miyazaki, Y., Kozyrev, I.L., Enose, Y., Shimada, T., Uesaka, H., Yamamoto, H., Miura, T., and Hayami, M. 1999. Protection of macaques against a SHIV with a homologous HIV-1 Env and a pathogenic SHIV-89.6P with a heterologous Env by vaccination with multiple gene-deleted SHIVs. Virology **265**: 252–263.
55) Ui, M., Kuwata, T., Igarashi, T., Miyazaki, Y., Tamaru, K., Shimada, T., Nakamura, M., Uesaka, H., Yamamoto, H., and Hayami, M. 1999. Protective immunity of gene-deleted SHIVs having an HIV-1 Env against challenge infection with a gene-intact SHIV. J. Med. Primatol. **28**: 242–248.
56) Winders, B.R., Schwartz, R.H., and Bruniquel, D. 2004. A distinct region of the murine IFN-gamma promoter is hypomethylated from early T cell development through mature naive and Th1 cell differentiation, but is hypermethylated in Th2 cells. J. Immunol. **173**: 7377–7384.
57) Wodarz, D., and Jansen, V.A. 2001. The role of T cell help for anti-viral CTL responses. J. Theor. Biol. **211**: 419–432.

Microbiol. Immunol., 49(7), 667–679, 2005

Editor-Communicated Paper

Intrathymic Effect of Acute Pathogenic SHIV Infection on T-Lineage Cells in Newborn Macaques

Hajime Suzuki[1], Makiko Motohara[1], Ariko Miyake[1], Kentaro Ibuki[1], Yoshinori Fukazawa[1], Katsuhisa Inaba[1], Kyoko Masuda[2], Nagahiro Minato[2], Hiroshi Kawamoto[3], Masanori Hayami[1], and Tomoyuki Miura*,[1]

[1]*Laboratory of Primate Model, Institute for Virus Research, Kyoto University, Kyoto, Kyoto 606–8507, Japan,* [2]*Graduate School of Biostudies, Kyoto University, Kyoto, Kyoto 606–8501, Japan, and* [3]*RIKEN Research Center for Allergy and Immunology, Yokohama, Kanagawa 230–0045, Japan*

Communicated by Dr. Hidechika Okada: Received April 22, 2005. Accepted April 25, 2005

Abstract: **We intrarectally infected newborn macaques with a pathogenic simian/human immunodeficiency virus (SHIV) that induced rapid and profound CD4$^+$ T cell depletion, and examined the early effects of this SHIV on the thymus. After intrarectal infection, viral loads were much higher in the thymus than in other lymphoid tissues in newborns. In contrast, no clear difference was seen in the viral loads of different tissues in adults. Histological and immunohistochemical observations showed severe thymic involution. Depletion of CD4$^+$ thymocytes began in the medulla at 2 weeks post infection and spread over the whole thymus. After *in vivo* infection, the CD2$^+$ subpopulation, which represents a relatively later stage of T cell progenitors, was selectively reduced and development of thymocytes from CD3$^-$CD4$^-$CD8$^-$ cells to CD4$^+$CD8$^+$ cells was impaired. These results suggest that profound and irreversible loss of CD4$^+$ cells that are observed in the peripheral blood of SHIV-infected monkeys are due to destruction of the thymus and impaired thymopoiesis as a result of SHIV infection in the thymus.**

Key words: **SHIV, Newborn, Thymopoiesis, Rhesus monkey**

The thymus is the primary organ of thymopoiesis and is highly active during early life. Clinical and experimental evidence suggests that the thymus is one of the important target organs for human immunodeficiency virus type 1 (HIV-1) infection (14, 37, 44). Histological studies of the thymus in HIV-1 infected children have revealed an association between abnormal morphological changes including thymic involution, thymocyte depletion and disruption of microenvironments and rapid progression of disease (3, 22, 31, 34). Although the initial interaction between virus and host is considered to be critical in the pathogenesis of HIV-1, detailed analysis of HIV-infected humans at the early phase of infection are extremely limited and nearly impossible to conduct serially (30, 40). Therefore, detailed studies of the thymus using animal models are needed to understand the pathogenicity of HIV.

HIV pathogenesis in the thymus has been investigated in several experimental models. In particular, thymic infection and destruction have been mainly investigated using simian immunodeficiency virus (SIV)/macaque and simian/human immunodeficiency virus (SHIV)/macaque models (16, 17, 26, 27, 41, 42, 45, 48) because the physical structure of monkeys and symptoms of induced immunodeficiency in monkeys are close to those of human. A great advantage of the SHIV/macaque model is that the SHIV contains the HIV *env* gene, which determines virus coreceptor usage

Address correspondence to Dr. Tomoyuki Miura, Laboratory of Primate Model, Experimental Research Center for Infectious Diseases, Institute for Virus Research, Kyoto University, 53 Shogoinkawara-machi, Sakyo-ku, Kyoto, Kyoto 606–8507, Japan. Fax: +81–75–761–9335. E-mail: tmiura@virus.kyoto-u.ac.jp

Abbreviations: AIDS, acquired immunodeficiency syndrome; CD4SP, CD3$^+$CD4$^+$CD8$^-$ single positive; CD8SP, CD3$^+$CD4$^-$CD8$^+$ single positive; DP, CD4$^+$CD8$^+$ double positive; dpi, days post-inoculation; FTOC, fetal thymus organ culture; HIV, human immunodeficiency virus; mAb, monoclonal antibody; PBMC, peripheral blood mononuclear cell; R5, CCR5; SHIV, simian/human immunodeficiency virus; SIV, simian immunodeficiency virus; $TCID_{50}$, 50% tissue culture infectious dose; TdT, terminal deoxynucleotidyl transferase; TN, CD3$^-$CD4$^-$CD8$^-$ triple negative; X4, CXCR4.

and cell tropism (19), and is a critical factor controlling replication in thymus (50).

Several SHIVs have been constructed and examined for infectivity in macaques (20, 28, 41, 47). After *in vivo* passage or anti-CD8 treatment, some of these viruses acquired acute pathogenicity, inducing profound $CD4^+$ T cell depletion and thymic atrophy in the early phase of infection (15, 21, 41, 49). Although this unusually rapid clinical course is not the same as that observed generally in HIV-1 infected humans, the symptoms of SHIV in monkeys have a number of similarities to the symptoms of HIV in humans. Acute pathogenic SHIVs that cause rapid and irreversible $CD4^+$ cell depletion in peripheral blood use CXCR4 (X4) only or in addition to CCR5 (R5) as its coreceptor for entry into susceptible cells (55). In HIV infection, X4-utilization is sufficient to trigger $CD4^+$ cell depletion in human tonsil tissue (38) and the emergence of X4-variants in HIV-infected patients is associated with accelerated progression to acquired immunodeficiency syndrome (AIDS) (4). Taken together, these results indicate that macaques infected with acute pathogenic SHIVs can be used as a model of individuals with emerging X4-utilizing HIV-1, which results in a rapid clinical course.

Although some investigators reported that thymic function might be impaired in HIV-1 infection (6, 12, 43), the effects of infection on the thymus have been controversial. The controversy could probably be resolved if an appropriate animal model and a method for directly measuring thymopoiesis could be found. Recent studies showed that in macaques inoculated with X4-utilizing viruses, massive depletion of peripheral naïve $CD4^+$ T cells was observed within 4 weeks of infection (36, 39). A critical role of the thymus is to supply naïve T cells to the peripheral blood during early life. Thus, a model using a combination of X4-utilizing SHIV and newborn macaques can be useful for clarifying the mechanism of the depletion of peripheral naïve $CD4^+$ T cells associated with thymic dysfunction.

We observed severe impairment of precursor function of $CD3^-CD4^-CD8^-$ triple negative (TN) cells at the early stage of infection with acute pathogenic SHIV in adult monkeys (unpublished data). However, because of thymic atrophy in adults, the morphological and functional changes that occur in the adult thymus as a result of viral infection are generally less informative than the changes that occur in the infant thymus (7). Therefore, to evaluate the effects of acute pathogenic SHIV infection on thymic function, we used newborn macaques to rule out the effect of age-related thymic atrophy. We intrarectally infected two newborns and sacrificed them at 13 days post-infection (dpi) and 26 dpi to carry out virological, biochemical and histopathological analyses. In addition, we examined the effects of aging and viral infection on T cell maturation, employing a fetal thymus organ culture (FTOC) system which is used to culture and develop rhesus monkey thymus progenitor cells in fetal mouse thymus lobe (35). The goals of the present study were to investigate the intrathymic effects of acute pathogenic SHIV (SHIV-C2/1) on T-lineage cells early after mucosal infection and to determine whether thymic dysfunction is related to the rapid clinical course observed in pediatric AIDS. We obtained two interesting results: (1) Virus loads were much higher in the thymus than in other lymphoid tissues in newborn macaques, but not in adults, and (2) thymopoiesis of TN cells was impaired at the early stage of infection.

Materials and Methods

Virus. KS661 is a molecular clone (GenBank ACCESSION No. AF217181) having a consensus sequence of the acute pathogenic SHIV-C2/1 strain, which was generated by *in vivo* passage of SHIV-89.6 (containing *env*, *tat*, *rev* and *vpu* derived from primary isolates of HIV-1 89.6 strain). SHIV-C2/1 was reported to infect macaque monkeys by intrarectal routes and to cause precipitous viremia and drastic depletion of $CD4^+$ cells (49). The virus stock was prepared from the supernatant of a human lymphoid cell line, CEMx174, and stored in liquid nitrogen until use. The 50% tissue culture infectious dose ($TCID_{50}$) of the virus stock was measured in CEMx174. Twenty $TCID_{50}$ was equivalent to one 50% macaque infectious dose (unpublished data).

Animal experiments. Thirteen rhesus macaque monkeys (*Macaca mulatta*) were used in this study. The monkeys included four newborns between 4 and 8 weeks of age at the time of sacrifice, four 3-year-old young macaques, and five adults between 6 and 8 years of age. The monkeys were housed in accordance with regulations approved by the Committee for Experimental Use and Care of Nonhuman Primate in the Institute for Virus Research, Kyoto University. Nine of the 13 monkeys (two of the newborns, all four of the young macaques and three of the adults) were inoculated intrarectally with 2×10^3 $TCID_{50}$ of SHIV-C2/1 KS661 after being anesthetized by intramuscular injection of ketamine chloride. All intrarectal inoculations were done with a pediatric feeding catheter to avoid causing trauma. The catheters were carefully inserted 5 cm into the anus of newborn monkeys and 10 cm into the anus of young and adult monkeys. These nine monkeys were euthanized as follows: One newborn was euthanized at each of 13 and 26 dpi. Two of the young

macaques were euthanized at 13 dpi and the other two were euthanized at 26 dpi. Two of the adult macaques were euthanized at 13 dpi and one adult macaque was euthanized at 27 dpi. The remaining four monkeys (two newborns and two adults) were used as age-matched uninfected controls.

Sample collection. Blood samples were periodically collected from all monkeys, treated with sodium citrate as an anticoagulant, and centrifuged to obtain plasma. Peripheral blood mononuclear cells (PBMCs) were separated from the buffy coat by Percoll (Lymphocyte Separation Solution; Nacalai Tesque, Kyoto, Japan) density gradient centrifugation. Separated plasma and PBMCs were stored at −80 C until use. Thymus, spleen and mesenteric lymph nodes were obtained at the time of necropsy, and minced and filtered through a 40 μm nylon filter (Becton Dickinson, Franklin Lakes, N.J., U.S.A.). These single cell suspension samples were divided and used for plaque assay and DNA extraction.

Measurement of viral loads. Plasma viral RNA levels were determined by real-time PCR (Prism 7700 Sequence Detector, Applied Biosystems, Foster City, Calif., U.S.A.) as described previously (27). The proviral DNA loads in PBMC and thymocytes were determined by quantitative PCR. RNA-free DNA samples were extracted from 2×10^6 cells with a QIAGEN DNeasy Tissue kit (QIAGEN, Hilden, Germany). PCR was performed with a Platinum qRT-PCR ThermoScript One-Step System (Invitrogen, Carlsbad, Calif., U.S.A.) using the same primer set and probe that were used in RT-PCR. A standard curve was generated from a plasmid DNA sample containing the full genome of KS661, which was quantified with a UV-spectrophotometer. Infectious viral roads in several lymphoid tissues were quantified using the infectious plaque assay as described previously (33).

Flow cytometry analysis. The frequency of $CD4^+$ T cells in whole bloods was examined as described previously (32). Thymocytes were stained for flow cytometry using the panel of monoclonal antibodies (mAbs) shown in Table 1. Cells were adjusted to a concentration of 10^6 cells/100 μl, stained using appropriately diluted antibody for 30 min at 4 C, washed, fixed with Cellfix (BD Biosciences, San Jose, Calif., U.S.A.), and analyzed with a FACScan or FACSCalibur analyzer (BD Biosciences). Thymocytes whose surface had already been stained were fixed with 1% formaldehyde, incubated with FACS permeabilization solution 2 (BD Biosciences) for 10 min, stained in the dark for 30 min with mAb against terminal deoxynucleotidyl transferase (TdT) or isotype-matched control (BD Biosciences), washed, resuspended in Cellfix and analyzed with the FACSCalibur analyzer.

Cell surface staining and cell sorting of obtained thymocytes. Cells were surface stained and TN cells were sorted as previously described (11). Thymocytes were stained with FITC-anti-monkey CD3, PE-anti-human CD4, APC-anti-human CD8 (Leu-2a; BD Biosciences) and 7-AAD Viability Dye (Coulter, Miami, Fla., U.S.A.). $CD3^-CD4^-CD8^-$ TN cells were sorted by FACSVantageSE (BD Biosciences). Non-lymphoid cells were excluded by forward and side scatters. Non-viable cells were excluded using 7-AAD Viability Dye. Sorted cells were reanalyzed to check their purity and were always found to be more than 99% pure.

Mice and fetal thymus organ culture (FTOC). Pregnant C57BL/6 (B6) mice were purchased from Japan SLC (Shizuoka, Japan). B6 fetuses (15 days post-coitum) were used in organ culture experiments as the source of fetal thymus lobes. Fetal thymus lobes were cultured as described previously (53) with subsequent modifications (23). One murine thymus lobe and 2,000 cells of $CD3^-CD4^-CD8^-$ TN monkey thymocytes purified by the cell sorter were added to each well into a total volume of 200 μl. Wells along the margin of the plate were not used, but filled with water to help maintain a high humidity in the plate. The plates were centrifuged at $150\times g$ for 5 min at room temperature, placed into a plastic bag (Ohmi Oder Air Service,

Table 1. Combinations of monoclonal antibodies used in the FACS analysis

Antibody combination	Labeled fluorescence			
	FITC[a]	PE[b]	PerCP[c]	APC[d]
1	CD2[e]	CD4[f]	CD3[g]	CD8[h]
2	CD11b[i]	CD4	CD3	CD8
3	CD16[j]	CD4	CD3	CD8
4	CD20[k]	CD4	CD3	CD8
5	CD4[f]	CD56[l]	CD3	CD8
6	TdT[m]	CD4	CD3	CD8

[a] Fluorescein isothiocyanate.
[b] Phycoerythrin.
[c] Peridinin chlorophyll protein.
[d] Allophycocyanin.
[e] Clone 39c1.5; Coulter, Miami, Fla., U.S.A.
[f] Clone Nu-Th/i; Nichirei, Tokyo.
[g] Anti-CD3 reagent (FN-18; Biosource, Camarillo, Calif., U.S.A.) was biotinylated, and a two-step staining procedure was performed using streptavidin PerCP (BD Biosciences Pharmingen) as the secondary reagent.
[h] Clone SK1; BD Biosciences, San Jose, Calif., U.S.A.
[i] Clone Bearl: Coulter, Miami, Fla., U.S.A.
[j] Clone 3G8; Coulter, Miami, Fla., U.S.A.
[k] Clone L27; BD Biosciences, San Jose, Calif., U.S.A.
[l] Clone B159; BD Biosciences, San Jose, Calif., U.S.A.
[m] Anti-terminal deoxynucleotidyl transferase reagent for detecting intracellular epitopes. It is a mixture of four monoclonal antibodies (HT1, HT4, HT8 and HT9; Beckman Coulter, Miami, Fla., U.S.A.).

Hikone, Japan), and the air inside was replaced by a gas mixture (70% O_2, 25% N_2 and 5% CO_2). The plastic bag was incubated at 37 C. The cultures were maintained in RPMI 1640 medium. The medium was changed every 2 or 3 days. Cells from both inside and outside the lobe were harvested from each well at each time point, and single cell suspensions were made. Viable cells were counted by trypan blue dye exclusion, and then surface phenotypes were analyzed by FACSVantageSE.

Histopathological and immunohistochemical examinations. The thymuses obtained from sacrificed monkeys were fixed in 4% paraformaldehyde and 1× phosphate-buffered saline overnight at 4 C, and then embed-

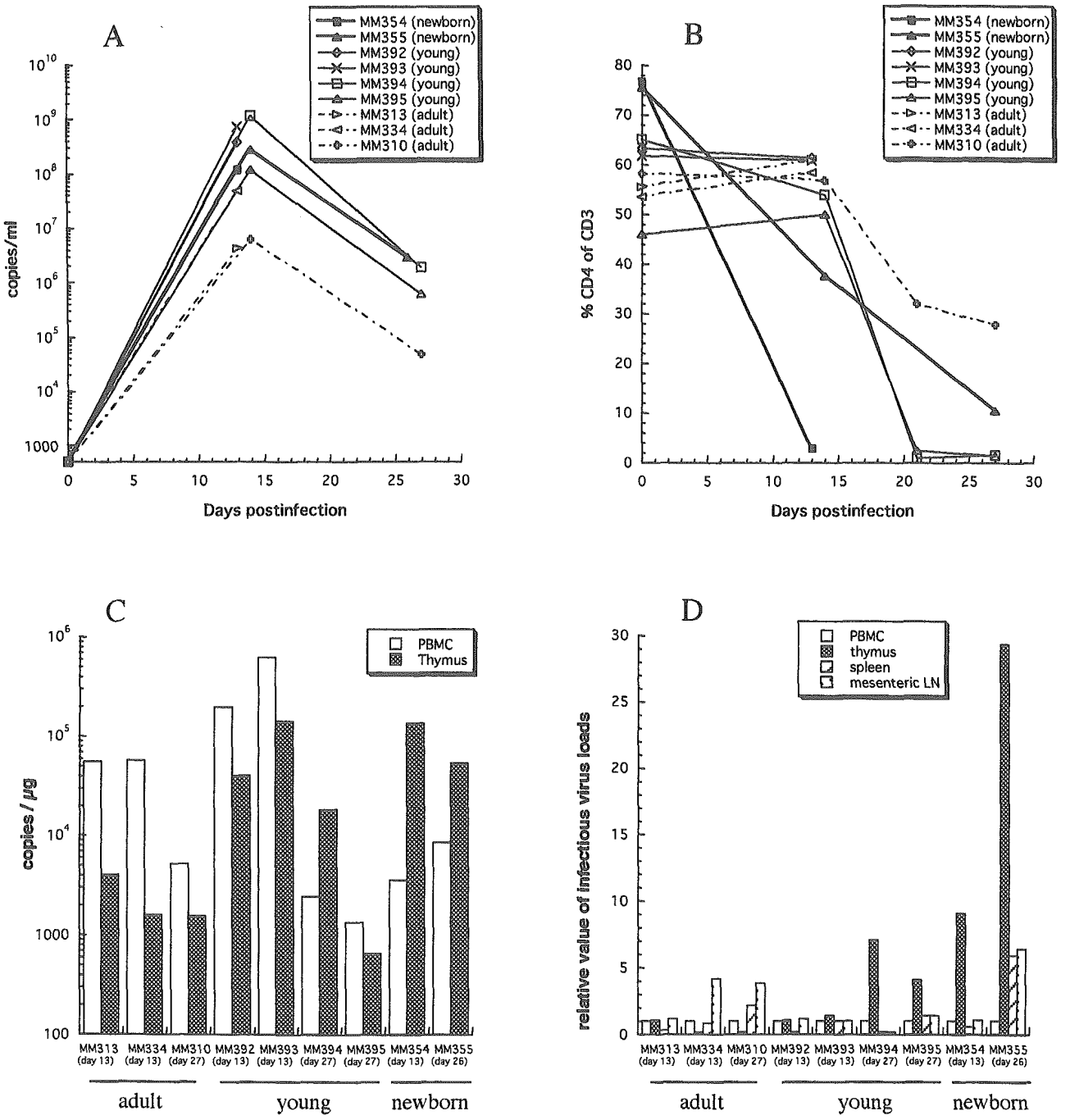

Fig. 1. Comparison of viral loads and $CD4^+$ T cell counts between newborn, young and adult macaques during acute SHIV-C2/1 infection. (A) Plasma viral RNA levels. (B) Relative frequency (percentage) of CD4 T cells. (C) Amounts of proviral DNA in PBMCs and thymus, as determined by quantitative PCR. Values are expressed as viral DNA copy numbers per microgram of total DNA extracted from single cell suspensions. (D) Infectious viral loads in lymphoid tissues relative to the viral load in PBMCs. Values were determined by infectious plaque assay.

ded in paraffin wax for histological (hematoxylin-eosin staining) and immunohistochemistry studies. Four-micrometer sections were dewaxed, pretreated by appropriate methods for each antibody (see below) and treated with TBS-Tween 20 and aqueous hydrogen peroxide. To stain CD4 antigen, sections were pretreated in 1 mM EDTA (pH 8.0) and autoclaved at 121 C for 15 min. To stain cytokeratin, sections were pretreated by proteinase K (Dako, Carpinteria, Calif., U.S.A.) at room temperature for 5 min. To stain ssDNA, sections were incubated overnight with 1% saponin at 4 C. To stain SIV-Nef antigen, sections were pretreated in 1 mM EDTA (pH 8.0) and autoclaved. Cells in the sections were stained with the following mAbs. $CD4^+$ cells were stained with anti-CD4 (NCL-CD4; Novocastra Laboratories, London, U.K.). Thymus epithelial cells were stained with anti-cytokeratin (MNF116; Dako, Carpinteria, Calif., U.S.A.). Apoptotic cells were stained with anti-ssDNA (Dako, Kyoto, Japan). Virus-positive cells were stained with anti-SIV Nef (aa 71–80; FIT Biotech Oyj Plc, Tampere, Finland) (51). Stained cells were visualized with an EnVision kit (Dako, Carpinteria, Calif., U.S.A.) and diaminobenzidine, rinsed in distilled water and counterstained with hematoxylin (Dako, Carpinteria, Calif., U.S.A.).

Results

Viral Loads and $CD4^+$ T Cells in Whole Blood

Plasma viremia of newborns reached a peak (more than 10^8 copies of RNA/ml) at 13 dpi and remained at high levels to 26 dpi. This pattern was similar to that in young and adult macaques (Fig. 1A). In all macaques, severe $CD4^+$ T cell depletion was observed within 4 weeks after inoculation (Fig. 1B). However, viral RNA levels were higher in newborn and young macaques at both 2 weeks and 4 weeks after inoculation than in adults, and were inversely correlated with $CD4^+$ T cell depletion. These data indicated that *in vivo* infectivity of acute pathogenic SHIV-C2/1 was higher in younger macaques.

The levels of proviral DNA in PBMCs and thymocytes were evaluated by performing quantitative PCR on the DNA extracted from suspensions of single cells. The proviral DNA loads in newborn thymus were highest at 13 dpi and remained at high levels to 26 dpi. In both of the infected newborns and in one of the four young macaques (MM394), the amounts of provirus were higher in thymocytes than in PBMCs. On the contrary, in all infected adults and in three of the four young macaques, the amounts of provirus were higher in PBMCs than in thymocytes (Fig. 1C). Infectious virus loads were considerably higher in thymocytes than in other lymphoid tissues in both of the infected newborns and in the two young macaques sacrificed at 27 dpi, although the amounts of infectious virus were not so different between thymocytes and other lymphoid tissues in the other infected macaques (Fig. 1D).

Alterations in the Phenotypes of Newborn Thymocytes

The profiles of lymphocyte subsets in the thymuses of the two infected newborns at 13 and 26 dpi were markedly different from the pattern observed in cells from the two uninfected controls (Table 2). As the infection period became longer, there were dramatic decreases of mature $CD3^+CD4^+CD8^-$ single positive (CD4SP) cells and immature $CD4^+CD8^+$ double positive (DP) cells and increases of immature $CD3^-CD4^-CD8^-$ triple negative (TN) cells and mature $CD3^+CD4^-CD8^+$ single positive (CD8SP) cells relative to the uninfected control. Of particular interest was the marked depletion of DP cells from about 90% to 5% and the relative increase of the percentage of TN cells from less than 1% to over 30%.

Impaired Thymopoietic Potential of $CD3^-CD4^-CD8^-$ TN Cells Due to Aging or Infection

We hypothesized that acute pathogenic SHIV infection prevents T cells from developing beyond TN cells, resulting in severe depletion of DP cells. To examine this hypothesis, we characterized the TN subsets, and evaluated the intrathymic effects of SHIV-C2/1 in more detail. The thymus is one of the most critical tissues for understanding acute pathogenicity, especially in infected newborn macaques. However, thymic function is known to be impaired with aging (1). Therefore, to better understand and to evaluate the effect of SHIV-C2/1

Table 2. Thymocyte subset changes in SHIV-C2/1-infected animals

Animal ID	% of cells				
	TN[a]	DP[b]	CD4SP[c]	CD8SP[d]	CD20
MM356 (uninfected)	0.2	90.1	7.7	1.4	<0.1
RM03 (uninfected)	0.9	86.0	9.8	1.2	0.3
MM354 (sacrificed 13 dpi)	1.1	94.2	**0.8**	1.5	<0.1
MM355 (sacrificed 26 dpi)	32.5	**5.1**	**0.9**	26.3	0.5

Values in bold represent a significant reduction and values with underbar represent a significant increase compared to uninfected controls.

[a] $CD3^-CD4^-CD8^-$ triple negative.

[b] $CD4^+CD8^+$ double positive.

[c] $CD3^+CD4^+CD8^-$ single positive.

[d] $CD3^+CD4^-CD8^+$ single positive.

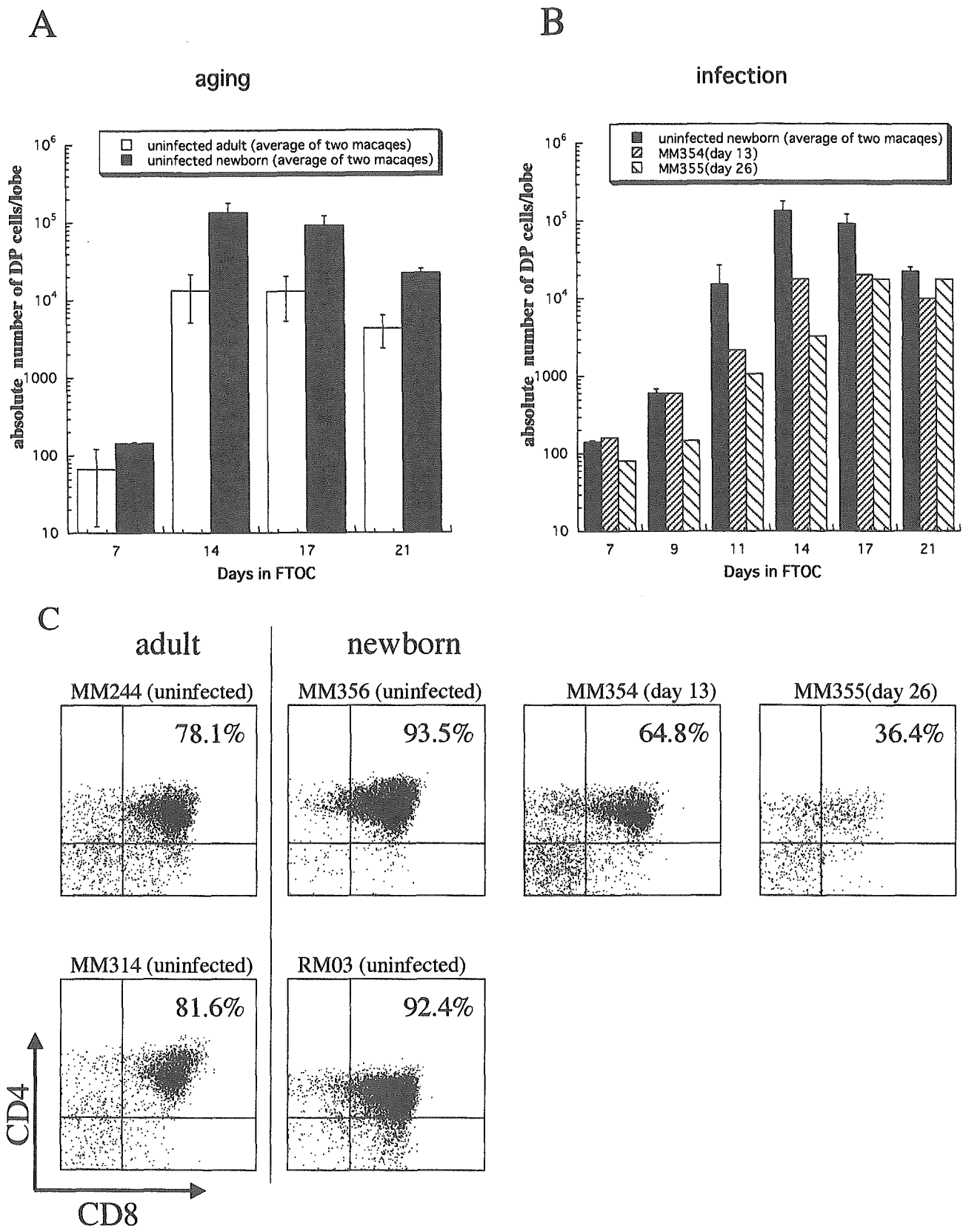

Fig. 2. Evaluation of progenitor function of $CD3^-CD4^-CD8^-$ triple negative (TN) subset in the thymus. (A) and (B) Abundance and growth kinetics of developed $CD4^+CD8^+$ double positive (DP) cells in FTOC. The absolute number of DP cells was the average cell numbers of three lobes. (A) Comparison of uninfected newborn and adult macaques to examine the effect of aging. (B) Comparison of uninfected and SHIV-C2/1-infected newborn macaques to examine the effect of infection. (C) Comparison of phenotypic maturation of TN cells into DP cells in uninfected and SHIV-C2/1-infected macaques at 14 days in FTOC.

on thymopoiesis, we must first understand the effect of normal thymic dysfunction (such as occurs as a result of aging or viral infection) on progenitor function of TN cells.

A monkey-mouse fetal thymus organ culture (FTOC) system is capable of reproducing the development of T cell progenitor from TN cells to DP cells *in vitro* (35). We evaluated the effects of aging or SHIV-C2/1 infection on T cell maturation during this period of development. The average peak absolute number of DP cells in the two uninfected adult macaques (MM244 and MM314) was about one-tenth that of uninfected newborn (MM356 and RM03). However, about 80% of the TN cells purified from uninfected adult macaques differentiated into DP cells after 14 days of FTOC (Fig. 2, A and C). In uninfected adults, 14 days of FTOC was enough to reach the peak level of differentiation, which is identical to the time required in uninfected newborns. These results suggest that thymic dysfunction by aging was due to a decrease in the number of progenitor cells that were able to develop into DP cells in the TN cells, rather than to the dysfunction that accompanies maturation of an individual progenitor.

To clarify the effect of viral infection, we compared the function of TN cells in SHIV-C2/1 infected newborns and age matched uninfected controls. The peak DP cell counts of both infected newborns (MM354 and 355) were as low as 1/7 the average of the peak DP cell counts of uninfected controls (MM356 and RM03). After 14 days of FTOC, the fractions of DP cells that differentiated from TN cells in MM354 (64.8%) and MM355 (36.4%) were lower than the fraction in uninfected newborns (over 90%). Fourteen days were required to reach the peak level of differentiation to DP cell counts in MM354 (sacrificed at 13 dpi) whereas 17 days was required to reach the peak level in MM355 (sacrificed at 26 dpi) (Fig. 2B). These data show that the effect of increasing the infection period was more to delay the differentiation than to decrease its peak level.

Phenotyping of CD3$^-$CD4$^-$CD8$^-$ TN Thymocytes

The SHIV-C2/1 infection caused a marked depletion of DP cells and a relative increase of TN cells, and impaired the thymopoietic potential of residual TN cells. We also examined the change in phenotype of TN cells. First, to evaluate the degree to which TN cells were contaminated by cells of non-T lineages, expressions of CD20 (B cells), CD11b (monocytes/macrophages), and CD16 and 56 (NK cells) were examined. Whole thymocytes from newborn macaques contained only small fractions of B cells (<1%), monocytes (<0.1%) and NK cells (<0.1%). These results indicated that the SHIV-infection did not bring about major changes to these subsets (data not shown). Second, thymocytes were stained with anti-CD2 mAb which is a marker of T cell precursors (7, 13, 52) or anti-TdT mAb which is a marker of lymphoid precursor cells (18, 29). After intrarectal infection with SHIV-

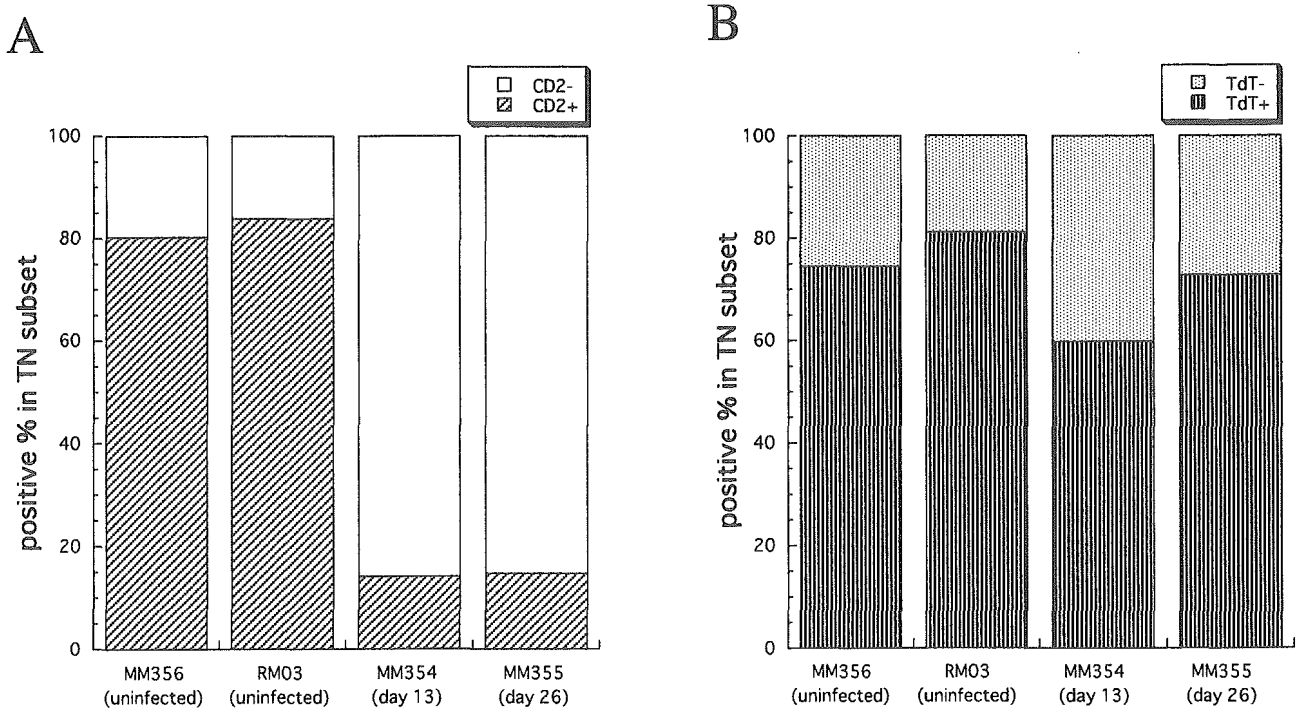

Fig. 3. Frequency of CD2$^+$ cells (A) and TdT$^+$ cells (B) in the TN subset during acute SHIV-C2/1 infection, as determined by flow cytometry. Thymocytes were obtained at the time of necropsy, and stained with mAbs to CD3, CD4, CD8 and CD2 or TdT.

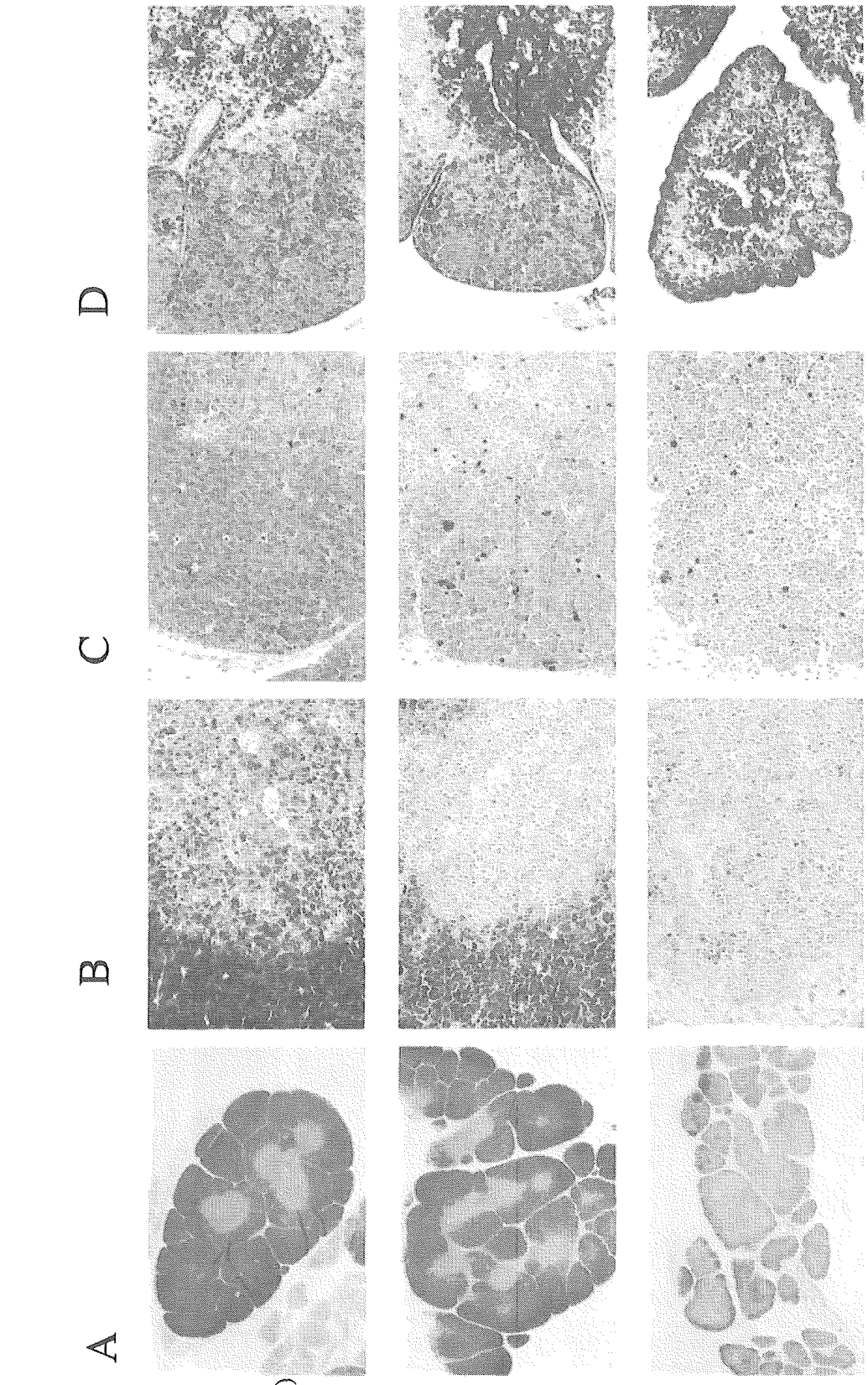

Fig. 4. Histopathological changes in thymus associated with acute SHIV-C2/1 infection. Sections of thymuses from an uninfected control macaque (MM356) as well as from newboms sacrificed at 13 dpi (MM354) and 26 dpi (MM355). Adjacent sections from the same tissue blocks were stained with (A) Hematoxylin and eosin (×40), (B) immunostained with anti-human CD4 mouse mAb (×100), (C) with single strand DNA to visualize apoptotic cells (×200) and (D) with anti-human cytokeratin mouse mAb to detect thymus epithelial cells (×100).

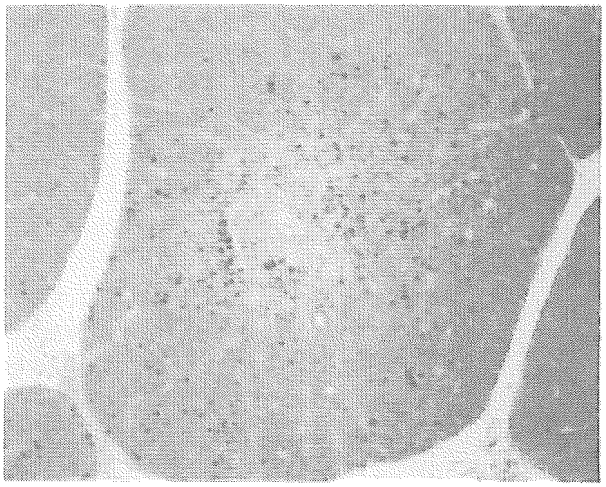

Fig. 5. Viral Nef$^+$ cells in a thymus from a newborn macaque infected with SHIV-C2/1 at 13 dpi (MM354). Thymus was immunostained with anti-SIV Nef antibody (×40).

C2/1, CD2$^+$ TN cells dramatically decreased from about 80% to 14% (Fig. 3A). By contrast, the fraction of TN cells that were TdT marker positive did not change very much after the infection (Fig. 3B).

Histopathological Analyses in the Thymus

To understand how the virus-infected thymus was altered in the early stage of infection, the SHIV-C2/1-infected thymuses were examined at 13 and 26 dpi. At 13 dpi, the thymus showed a thinning of the cortex in some lobules and mildly increased white spots like starry sky, which are tingible-body macrophages in the cortex (Fig. 4A, middle). Expansion of the medulla was observed with infiltration of neutrophilic inflammatory cells and mildly decreased density of thymocytes. The depleted cells were identified as CD4$^+$ cells by immunohistochemical examination (Fig. 4B, middle). Subsequently, the continuous progression of thymic involution resulted in small, atrophic lobules widely separated by prominent interlobular connective septa with no visible thymic cortex and no discernible corticomedullary junction at 26 dpi (Fig. 4A, bottom). The staining properties and location of apoptotic cells that were positive for single stranded DNA (DNA fragmentation) in the thymus of uninfected and infected animals are shown in Fig. 4C. At 13 dpi, apoptotic signals were increased particularly in the cortex. These signals were consistent with tingible-body macrophages which were considered in the process of phagocytosing apoptotic cells (Fig. 4C, middle). On day 26, apoptotic cells were decreased (Fig. 4C, bottom). Crosstalk between thymocytes and thymus epithelial cells is thought to be important for thymopoiesis (46). Therefore, we tested for the presence of cytokeratin-immunopositive epithelial cells. These cells were found to become more prominent in the thymus lobe with increasing infection period (Fig. 4D). These results indicate that the epithelial framework remained in the infected thymus, although acute thymic involution with severe depletion of thymocytes was observed. In the thymus of the SHIV-C2/1-infected newborn examined at 13 dpi, immunohistochemical staining showed that the majority of virus Nef$^+$ cells were located in the medulla or the corticomedullary junction, although a small number of Nef$^+$ cells were also present in the cortex (Fig. 5).

Discussion

This study demonstrated that intrarectal infection with SHIV-C2/1 caused a rapid and profound depletion of peripheral CD4$^+$ T cells in newborn rhesus macaques, as was previously observed to occur in young and adult macaques. However, in newborn macaques, viral loads in the thymus were much higher than those in other tissues, whereas no clear difference of viral loads was observed among lymphoid tissues in adults, and intermediate results were observed in young macaques (Fig. 1, C and D). These results indicate that the distribution of virus in different tissues in the newborns early after mucosal infection was considerably different from that in adults. Since membrane fluidity influences the HIV-1 infectivity (9, 10), it may be interesting to determine the plasma membrane fluidity of infant thymocytes.

We employed a monkey-mouse FTOC system to evaluate the progenitor function of TN cells. This assay can directly measure thymopoiesis in the immature stage. TN cells isolated from newborns produced more CD4-expressing cells in FTOC than did TN cells isolated from adults (Fig. 2A). That is, the thymus of newborns can supply a greater number of virus target cells than can the thymus of adults. Taken together, these findings suggest that the thymus is a major site of viral replication and an important target organ in the pathogenicity of AIDS in newborns. Table 2 shows that severe DP cell depletion occurred at 26 dpi. This result and the histological results are similar to what was observed in a newborn human with congenital HIV-1 infection (44). The thymus of this individual showed severe depletion of both CD4 single positive and DP subsets.

In previously studied SIV infections, the depletion of DP cells was temporary (between 14 and 21 days). In contrast, the depletion of DP cells was stable in SHIV-infected monkeys, although there was an increase of apoptotic thymocytes coincident with the peak of SIV-viremia similar to SHIV-infected monkeys (45). This

difference suggest that some mechanism other than direct killing and apoptosis is responsible for the depletion of DP cells. A recent study demonstrated that HIV infection caused a rapid and sustained suppression of thymocyte proliferation (5). This study used an indirect assay in PBMCs, based on the ratio of different T cell receptor excision circles, which are molecular markers of distinct T cell rearrangements occurring at different stages of T cell development. In the present study, we directly measured thymopoiesis using the FTOC system, and showed that SHIV-C2/1 infection impaired progenitor function of the thymocytes. The impairment was of the progenitor itself, and not due to the destruction of the thymic environment that is indispensable to thymopoiesis, because the xenogeneic FTOC used mouse stroma that are non-sensitive to SHIV infection.

MM354 (at 13 dpi) showed considerable depletion of mature CD4 single positive cells (Table 2) and mild thymic atrophy with $CD4^+$ cell depletion in the medulla (Fig. 4, A and B, middle panels). Most of the virus-infected cells were localized in this area (Fig. 5). At the same time in the FTOC, the ability of TN cells in the thymus to differentiate to DP cells was already impaired (Fig. 2B), although the FACS analysis detected no appreciable change in DP subsets in the thymus (Table 2). At 26 dpi (MM355), DP cells were severely depleted (Table 2) and the cortex region in the thymus disappeared (Fig. 4A, bottom panel). Immature thymocytes are mainly present in the cortex, whereas mature thymocytes are mainly present in the medulla (2). That is, an impaired thymopoiesis measured by FTOC is predictive of DP cell depletion in the thymus *in vivo*. Taken together, these results indicate that the early stage of infection in newborn macaques infected intrarectally with SHIV-C2/1 has two phases. The first phase is direct infection and active replication in mature $CD4^+$ cells that result in the depletion of mature CD4 single positive cells in the thymus that was observed at 13 dpi. The thymus in this phase is probably the main source of the virus production causing the peak of plasma viremia. The second phase, which was observed at 26 dpi, after the peak of plasma viremia, is the immature cell depletion phase and was caused by the impairment of thymopoiesis. These data also indicate that SHIV-C2/1 infection affects immature thymocytes, especially as the infection period became longer.

In this study, we showed impaired thymopoietic potential of TN cells from acute SHIV-C2/1-infected macaques. Neben et al. showed that the thymopoietic potential of $CD3^-CD4^+CD8^-$ cells, but not TN cells, was impaired in the acute phase of SIV infection (35). *De novo* generation of naïve T cells occurs in the thymus after progenitors migrate from bone marrow. These progenitor cells differentiate from TN into $CD3^-CD4^+CD8^-$ cells and in the next step into DP cells. That is, SHIV-C2/1 infection affects T cell development in the thymus at earlier stage than does SIV infection *in vivo*. We previously observed a greater number of virus-expressing cells in thymuses infected with acute pathogenic SHIV than in thymuses infected with SIV at the early stage of intravenous infection (48). A histopathological study of pathogenic SHIV-infected thymus showed differences in thymic pathology based on coreceptor usage controlled by the HIV-1 env gene. The thymic atrophy associated with X4-utilizing SHIV was more severe than that of R5-utilizing SHIV (42). The thymus of the newborn examined at 26 days after infection with SHIV-C2/1 (which uses X4 in addition to R5) showed severe thymic atrophy with depletion of cortical cells. Similar symptoms were observed in an infant monkey infected with an X4-utilizing SHIV (42). SIV generally uses R5 rather than X4 as a coreceptor. Taken together, these results suggest that utilization of X4 as the coreceptor is highly associated with the thymus tropism and that the virus burden in the thymus is the key factor impairing the progenitor function of TN cells *in vivo*.

Both infected newborn macaques showed a reduced number of differentiated DP cells in FTOC compared with the uninfected controls (Fig. 2B). While determining the culture conditions for the FTOC, we noticed that if we used less than the normal number of cells (2,000) in the uninfected control experiment, the peak levels of differentiated DP cell counts were reduced, although the time to reach the peak was the same as it was when 2,000 cells were used (14 days) (data not shown). Since the time to reach the peak level of DP cell counts of MM354 (14 days) was the same as that in the uninfected controls, the impairment of thymopoiesis as a result of SHIV-C2/1 infection at 13 dpi could be attributed to the quantitative decrease of the subpopulation of TN cells that are able to differentiate to DP cells in FTOC. On the other hand, MM355 took more time (17 days) to reach the peak, although the peak level of DP cell counts was almost the same as that in MM354. This result suggests that the proliferation ability of TN cells at 26 dpi is impaired by poor functioning of the cells. This impairment is in addition to the impairment at 13 dpi, which is mostly due to a decrease in the number of functional progenitor cells. FACS analysis of the TN cell population showed selective reduction of $CD2^+$ TN subsets (Fig. 3A). The sequence of development of thymocytes is $CD2^-TN \rightarrow CD2^+TN \rightarrow CD3^-CD4^+CD8^- \rightarrow DP$ in the early stages of thymic T-cell ontogeny (8, 25). Taken together, these data suggest that the $CD2^+TN$ subset is